Siberian Branch of Russian Academy of Science
BUDKER INSTITUTE OF NUCLEAR PHYSICS

B.V. Chirikov and V.G. Davidovsky

DYNAMICS OF A SIMPLE MODEL FOR TURBULENCE OF THE SECOND SOUND IN HELIUM II

Budker INP 99-70

http://www.inp.nsk.su/publications

Novosibirsk
1999

Siberian Branch of Russian Academy of Science
BUDKER INSTITUTE OF NUCLEAR PHYSICS

B.V. Chirikov and V.G. Davidovsky

DYNAMICS OF A SIMPLE MODEL FOR TURBULENCE OF THE SECOND SOUND IN HELIUM II

Budker INP 99-70

NOVOSIBIRSK
1999

Dynamics of a Simple Model for Turbulence of the Second Sound in Helium II

B.V. Chirikov and V.G. Davidovsky

Budker Institute of Nuclear Physics
630090 Novosibirsk, Russia

Abstract

The results of numerical experiments on chaotic ('turbulent') dynamics of the second sound in helium II are presented and discussed based on a very simple model proposed and theoretically studied recently by Khalatnikov and Kroyter. Using a powerful present–day techniques for the studying nonlinear phenomena, we confirm their results on the stationary oscillation in helium and its stability as well as on a qualitative picture of successive transitions to limit cycles and chaos. However, the experiments revealed also a much more complicated structure of the bifurcations than it was expected. The fractal structure of chaotic attractors was also studied including their noninteger dimension. Surprisingly, a very simple model used in all these studies not only qualitatively represents the behavior of helium in laboratory experiments but also allows for a correct order–of–magnitude estimate of the critical heat pumping into helium at bifurcations.

Email: chirikov@inp.nsk.su
Email: davidovsky@inp.nsk.su

1 Introduction

The present studies were stimulated by the theoretical analysis of the dynamics of the second sound in helium driven by the external heat periodic perturbation [1]. In turn, this theory was developed to explain the experiments on the second sound propagation in a liquid helium with a free surface [2, 3]. Originally, such experiments were intended for a new scheme of holography using the deformation of the helium surface under the standing waves in the bulk of the liquid [4]. To the best of our knowledge, such a project was never realized. The reason is very simple: a negligible surface deformation which is determined by the oscillation of the pressure in a second–sound wave, which is much smaller than the temperature oscillation. Nevertheless, the experiments were continued, and an interesting dynamics was observed, namely the transition, at a sufficiently high heat pumping into the helium, from a stationary second–sound wave to its chaotic motion, or turbulence [3]. This was just the subject of the theoretical analysis in Ref.[1]. The latter was necessarily restricted, even in the simplest model considered, to the calculation of the stability of a stationary standing wave. For this reason the authors [1] began also some numerical experiments which qualitatively confirmed their conjecture on a transition to limit cycles and chaos. The main purpose of our numerical studies is to continue such experiments for a more detailed and reliable analysis of those transitions.

2 The model

We adopted the model developed in Ref.[1] which can be specified by the following effective non–Hermitian Hamiltonian (in notations of Ref.[1] with only a few minor modifications):

$$H(a_1, a_2, t) = (\omega_1 - i\gamma_1)|a_1|^2 + (\omega_2 - i\gamma_2)|a_2|^2 + (\lambda a_1^2 a_2^* + f a_1^* e^{-i\omega t} + \text{c.c.}) \tag{2.1}$$

This Hamiltonian describes the two wave modes (oscillators) via complex phase–space variables a_j $(j = 1, 2)$ and the complex small–oscillation frequencies $\omega_j - i\gamma_j$ with phenomenological dissipation parameters γ_j. Two other parameters of the model, representing some effective nonlinear coupling of the two modes λ and the driving 'force' (external heat pumping) f of frequency ω, can be chosen real and positive. The model parameter f is related to the input heat power by an approximate expression

$$P \approx \frac{\partial H}{\partial t} = -2f\omega\,\mathrm{Im}(\bar{a}_1) \tag{2.2}$$

provided the parameters γ_j and f are sufficiently small. Here $\bar{a}_j$ are the new variables ('slow' amplitudes of the wave modes) determined by the canonical transformation

$$\begin{aligned} a_1 &= \bar{a}_1 e^{-i\omega t} \\ a_2 &= \bar{a}_2 e^{-2i\omega t} \end{aligned} \tag{2.3}$$

which eliminates the explicit dependence on time in Eq.(2.1). Below we omit the upper bar in all a_j. Notice that the new Hamiltonian still exactly describes the original model (2.1). The corresponding motion equations have the form:

$$\begin{aligned} i\dot{a}_1 &= (\Delta_1 - i\gamma_1)a_1 + 2\lambda a_1^* a_2 + f \\ i\dot{a}_2 &= (\Delta_2 - i\gamma_2)a_2 + \lambda a_1^2 \end{aligned} \tag{2.4}$$

where $\Delta_1 = \omega_1 - \omega$ and $\Delta_2 = \omega_2 - 2\omega$ are the detunings of the small–amplitude oscillation frequencies with respect to that of the driving force.

The described model is actually the simplest possible one for representing a complicated dynamics of the real physical system under consideration. Particularly, only the lowest (third–order in Hamiltonian) nonlinear term is included. Meanwhile, the next, fourth–order term is known to give a comparable contribution, particularly to the nonlinear shift of the oscillation frequencies. In Ref.[1] an argument is given for neglecting this term. In our opinion, the main argument is in that the next term does not lead to new qualitative effects, and moreover retains the order–of–magnitude of the description which is the best one could expect from such a primitive model. In any event, following Ref.[1] we also restrict our studies to the equations (2.4).

3 Numerics

In numerical experiments the set of equations (2.4) was integrated by itself (for trajectories) or together with the linearized equations (for Lyapunov exponents) using the Fehlberg version of the forth–order Runge - Kutta algorithm. A typical integration step was $\Delta t \sim 2^{-18}$. The accuracy of integration was checked, as usual, by a change of the step size. In case of a stable motion (stationary oscillation, limit cycle) the criterion of accuracy was a negligible change of the trajectory. However, for chaotic motion this was never possible, and we checked instead the accuracy of statistical properties of the motion, for example of the Lyapunov exponents.

We computed all (4) exponents Λ_n $(\Lambda_{max} \equiv \Lambda_1 \geq \Lambda_2 \geq \Lambda_3 \geq \Lambda_4)$ using also the standard method (see, e.g., Ref.[5]). One of them, whose eigenvector goes along the trajectory, is always zero while the sum of all

$$\Lambda_\Gamma = \sum_{n=1}^{4} \Lambda_n = -2(\gamma_1 + \gamma_2) = \text{const} \tag{3.1}$$

is the rate of the phase space volume contraction. Both conditions were also used to check the integration accuracy.

All the model parameters but f were fixed to (in CGS units)

$$\begin{aligned} &\Delta_1 = 0 \quad &&\Delta_2 = -1500 \\ &\gamma_1 = 30 \quad &&\gamma_2 = 120 \\ &\lambda = 5400 \quad &&\text{and} \\ &\omega = 8000 \end{aligned} \tag{3.2}$$

as in Ref.[1]. The principal parameter λ was calculated in Ref.[6]. The rest were chosen close to those in a typical laboratory experiment [2, 3]. We add also the driving frequency ω [2], absent in Eq.(2.4), which we will need below for a quantitative comparison with the laboratory experiments. The remaining parameter f, related to the input heat power (see Eq.(2.2)), was the only varying one in this first series of our numerical experiments.

In agreement with laboratory experiments the initial conditions were fixed at

$$a_1(0) = a_2(0) = 0 \tag{3.3}$$

which is important for the interpretation of numerical experiments below.

The main results of our experiments are presented in Fig.1 as a dependence of the maximal Lyapunov exponent $\Lambda_{max}(f)$ on the driving parameter f.

Three qualitatively different regimes of the motion are clearly seen:

(i) $\Lambda_{max} < 0$ and, hence, all Λ's are negative. This means a stationary standing wave according to the original Hamiltonian (2.1) or the constant amplitudes (a_j =const) in the reduced motion equations (2.4) that is a fixed point in the amplitude space. This is the simplest regime well recognized in both laboratory and numerical experiments.

(ii) $\Lambda_{max} = 0$. This may be a periodic (limit cycle) or quasiperiodic attractor. In the former (simplest) case the trajectory is closed. One way to recognize the cycle is simply to see a picture of the trajectory, or rather of some two–dimensional representation of the four–dimensional trajectory. This was done in Ref.[1], and we will not repeat it here. However, in case of a quasiperiodic attractor this visual analysis doesn't work.

(iii) $\Lambda_{max} > 0$. This is the most simple and reliable criterion for chaotic motion. The visual difference between the chaotic attractor and a complicated limit cycle is not always clear and may be deceptive.

As the force f grows the first very sharp bifurcation (fixed point/limit cycle) occurs at $f_1 \approx 97$ but it does not mean the fixed–point attractor disappears for larger f. Indeed, both the theory [1] and our numerical experiments show that the attractor retains up to $f \approx 380$ for some initial conditions of the motion which are generally different from (3.3). What actually happens in the first bifurcation is the escape of the initial point (3.3) out of the basin of attraction [1]. Particularly, this explains the 'window' with a fixed–point attractor at larger $f \approx 137 - 185$ (Fig.1).

At still greater $f = f_2 \approx 461$ a new and much more interesting bifurcation occurs (limit cycle/chaotic attractor). Actually, it is a complicated chain of many bifurcations between periodic and chaotic attractors. This is especially clear in Fig.2 where a narrow part of dependence $\Lambda_{max}(f)$ is shown in detail (cf. Fig.1).

The structure of each chaotic attractor is rather intricate, and particularly fractal. An important characteristic of such a structure is the dimension which is generally noninteger (see, e.g., Ref.[5]). The dimension can be calculated from the Lyapunov exponents using the relation

$$d = m + \frac{\sum_{n=1}^{m} \Lambda_n}{|\Lambda_{m+1}|} \qquad (3.4)$$

where m is the largest integer for which the sum $S_m = \sum_{n=1}^{m} \Lambda_n \geq 0$. This is the simplest and widely used method for calculating the dimension. For

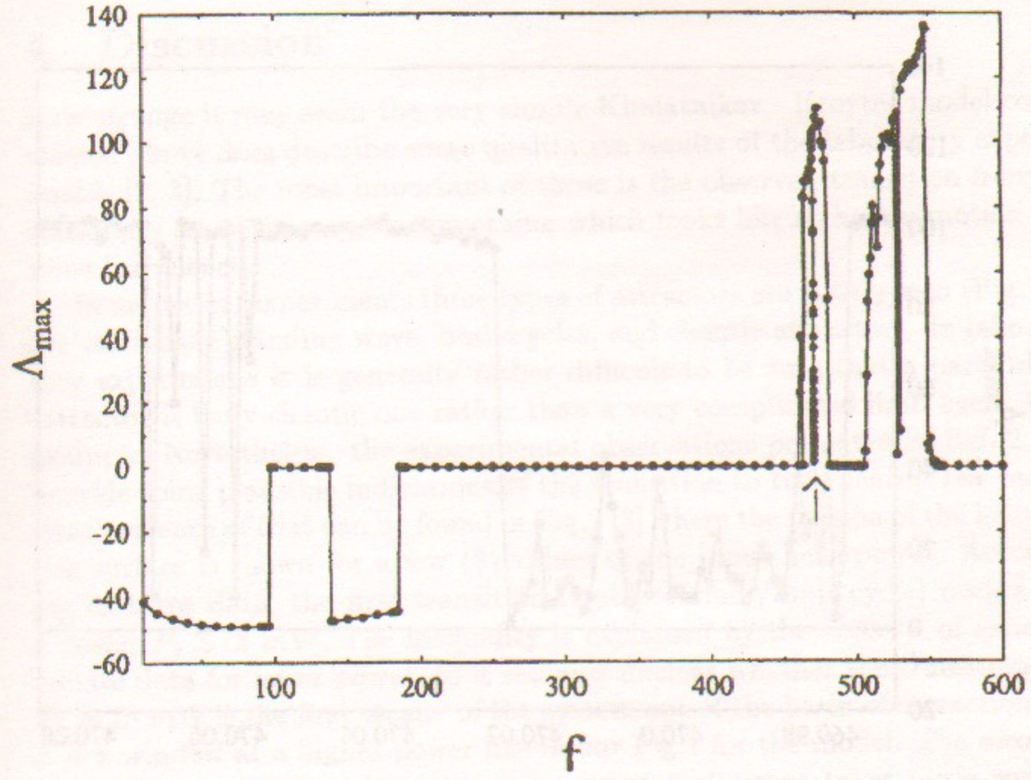

Figure 1: The global dependence of the maximal Lyapunov exponent Λ_{max} on the driving force f revealing the three types of attractor in model (2.4) with parameters (3.2) and initial conditions (3.3). Empirical points are connected by line to guide the eye.

example, on a fixed–point attractor (all Λ's are negative) $m = 0$, and $d = 0$. Similarly, for a periodic attractor (limit cycle) $m = 1$, and $d = 1$ (a closed trajectory). In case of a quasiperiodic attractor $m = d = 2$ or 3, so that the trajectory is asymptotically restricted to a phase–space surface of dimension 2 or 3, respectively. We tried but couldn't find any quasiperiodic attractor in the model under cosideration.

Unlike this, the dimension of a chaotic attractor is fractal because two of the four Lyapunov exponents are independent. In principle, three different cases are possible: (i) $\Lambda_2 = 0$ ($\Lambda_1 > 0$); (ii) $\Lambda_3 = 0$ ($\Lambda_1 \geq \Lambda_2 > 0$); and (iii) $\Lambda_2 = \Lambda_3 = 0$ ($\Lambda_1 > 0$). In our experiments we have always seen the first case only and never the two latter ones.

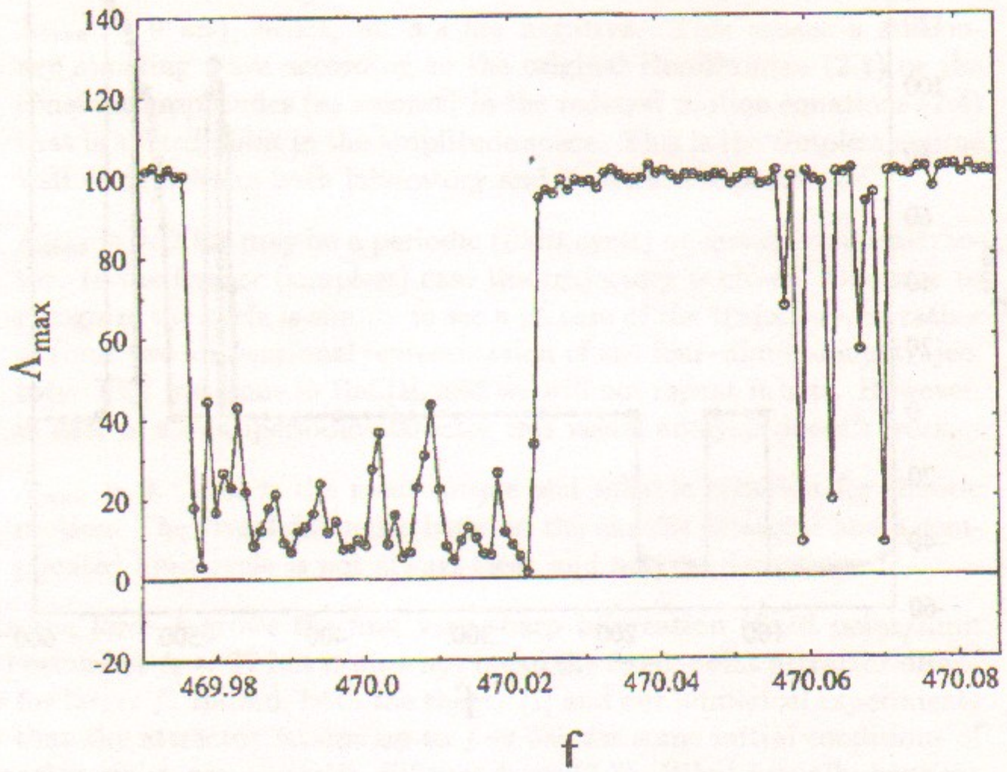

Figure 2: Same as in Fig.1 for a very narrow interval of f, indicated by arrow, where a deep drop of $\Lambda_{max} > 0$ occurs.

In the experiments presented in Fig.1 for $f \leq 600$ ($\Lambda_1 \leq 140$) the attractor dimension was in the interval ($2 < d < 3$) corresponding to $m = 2$ and $S_m = \Lambda_1$ (see Eq.(3.4)). For larger f the dimension grows due to increase of m ($S_m = S_3 = \Lambda_1 + \Lambda_3 \geq 0$), and can be represented in the form:

$$d(S_3) = 3 - \frac{S_3}{\Lambda_4} = 3 + \frac{S_3}{|\Lambda_\Gamma| + S_3} < 4 \qquad (3.5)$$

In agreement with the physical meaning of the dimension it never exceeds the upper bound $d_{max} = 4$. Whether d is actually approaching this bound is an interesting question. However, it makes sense for the model only, since at such a big f the model becomes certainly inadequate for the real physical system under consideration.

The above analysis of attractors in the model was confirmed by the computation of the motion spectra and correlation functions.

4 Discussion

How strange it may seem the very simple Khalatnikov - Kroyter model considered above does describe some qualitative results of the laboratory experiments [2, 3]. The most important of those is the observed transition from a stationary standing wave to something which looks like a chaotic motion or wave turbulence.

In numerical experiments three types of attractors are clearly seen (Fig.1): the stationary standing wave, limit cycles, and chaotic attractors. In laboratory experiments it is generally rather difficult to be sure that a particular attractor is truly chaotic one rather than a very complicated limit cycle, for example. Nevertheless, the experimental observations presented in Ref.[2, 3] provide some plausible indications of the transition to turbulence. The most clear evidence of that can be found in Fig.2 [3] where the motion of the helium free surface is shown for a few (3) values of the input heat power. According to these data, the first transition (stable surface/limit cycle) occurs at a power $P_1 \lesssim 18$ mW. The inequality is explained by the absence of experimental data for lower power, so it remains unclear whether the transition at $P_1 \approx 18$ mW is the first escape of the system out of the basin of attraction or it is a window at a higher power like in our Fig.1 for the model. The second (most interesting) transition to an apparent turbulence takes place somewhere in the interval $P_2 \approx 18 - 93$ mW. Here we take the lower P_2 equal to the upper P_1 for the same reason, the absence of intermediate experimental data.

In the model, the critical power input can be estimated from Eq.(2.2) as

$$P_1 \approx 2.6 \text{ mW} \quad \text{at} \quad f \approx 95, \ \text{Im}(a_1) \approx -0.016 \qquad (4.1a)$$

for the first transition and the first escape out of the attraction basin (see Fig.1) or

$$P_1 \approx 4.8 \text{ mW} \quad \text{at} \quad f \approx 170, \ \text{Im}(a_1) \approx -0.018 \qquad (4.1b)$$

for the second escape. As to the transition to a chaotic attractor, the critical power in the model is

$$P_2 \approx 26 \text{ mW} \quad \text{at} \quad f \approx 450, \ \text{Im}(a_1) \approx -0.036 \qquad (4.1c)$$

In such a simple model it seems to be a quite reasonable agreement (especially for the transition to turbulence), and in view of a considerable uncertainty in laboratory experiments.

The success of the Khalatnikov - Kroyter model can be explained, at least partly, by the special choice of the parameters of experiments when one of

the wave modes was in resonance with the input heat oscillation. Since the dissipation in higher modes is rapidly increasing, only a few lower modes are excited initially which turned out to be already sufficient for the transition to turbulence. For a higher power input the number of excited modes also rapidly grows, and the model becomes inadequate.

An interesting question about the maximal dimension of a chaotic attractor in the model (see Section 3), being irrelevant for the physical model under consideration here, may still be of importance for the theory of dissipative dynamical systems, and deserves further studies.

Acknowledgments. We are grateful to I.M. Khalatnikov for attracting our attention to this interesting physical problem, and for providing an opportunity to acquaint ourselves with his and M. Kroyter's results prior to publication. We appreciate many interesting and stimulating discussions with both of them.

References

[1] I.M. Khalatnikov and M. Kroyter, Zh. Eksp. Teor. Fiz. **115**, 1137 (1999); M. Kroyter, Master thesis, School of Physics and Astronomy, Tel-Aviv University (1998).

[2] J.L. Olsen, J. Low Temperature **61**, 17 (1985).

[3] P.W. Egolf, J.L. Olsen, B. Roehricht and D.A. Weiss, Physica **B169**, 217 (1991).

[4] J.L. Olsen, Helv. Phys. Acta **46**, 35 (1973); Physica **69**, 136 (1973).

[5] A. Lichtenberg and M. Lieberman, *Regular and Chaotic Dynamics*, Springer (1992).

[6] I.M. Khalatnikov, G.V. Kolmakov, V.L. Pokrovsky, JETP **107**, 1563 (1995).

B.V. Chirikov and V.G. Davidovsky

Dynamics of a simple model for turbulence of the second sound in helium II

В.Г. Давидовский, Б.В. Чириков

Динамика простой модели турбулентности второго звука в гелии II

Budker INP 99-70

Ответственный за выпуск А.М. Кудрявцев
Работа поступила 25.08.1999 г.

Сдано в набор 2.08.1999 г.
Подписано в печать 3.08.1999 г.
Формат бумаги 60×90 1/16 Объем 1.8 печ.л., 1.5 уч.-изд.л.
Тираж 130 экз. Бесплатно. Заказ № 70

Обработано на IBM PC и отпечатано на
ротапринте ИЯФ им. Г.И. Будкера СО РАН
Новосибирск, 630090, пр. академика Лаврентьева, 11.